Turk J Gastroenterol *2016; 27: 257-63*

Hepatic pathology of biliary atresia: A new comprehensive evaluation method using liver biopsy

BILIARY

Shouhua Zhang[1], Yan Wu[2], Zhiwen Liu[1], Qiang Tao[1], Jinshi Huang[1], Wenping Yang[2]

[1]Department of General Surgery, Jiangxi Children's Hospital, Nangchang, China
[2]Department of Pathology, Jiangxi Children's Hosptial, Nangchang, China

Original Article

ABSTRACT

Background/Aims: Despite its unique pathological characteristics, biliary atresia (BA) has no consensus pathological grading system. Therefore, the purpose of this study was to propose a new pathological grading system and to compare the diagnostic value of intraoperative frozen and postoperative paraffin-embedded liver sections.

Materials and Methods: A total of 81 BA patients were analyzed for clinical and biochemical data, immunohistochemistry, and routine postoperative histology and intraoperative frozen pathology sections. Bile duct hyperplasia was classified into three grades (B1–B3), and fibrosis was classified into four classical grades (F1–F4).

Results: The patients included 41 males and 40 females, aged 35–150 days. The repartition, in terms of severity, of small bile duct hyperplasia and fibrosis was as follows: B1, 21 cases; B2, 41 cases; B3, 19 cases; F1, 1 case; F2, 11 cases; F3, 51 cases; and F4, 18 cases. Both grades were statistically correlated. When comparing intraoperative frozen and postoperative paraffin-embedded sections, the overall diagnostic concordance rate was 97.5%.

Conclusion: The new proposed pathological grading system may be useful for the diagnostic and prognostic assessment of BA. In addition, intraoperative frozen liver tissue biopsy samples represent a valuable and promising adjunct to the conventional postoperative paraffin-embedded sections.

Keywords: Biliary atresia, liver tissue biopsy, intraoperative frozen pathology

INTRODUCTION

Biliary atresia (BA) is one of the main pediatric causes of persistent jaundice with progressive liver fibrosis, eventually leading to biliary cirrhosis (1). BA has its own special pathological characteristics, consisting particularly of intrahepatic cholestasis with bile plug formation, small bile duct hyperplasia, inflammatory cell infiltration, and fibrosis in the portal tracts. However, a grading system for the comprehensive evaluation of pathological changes is still lacking. Kasai cholangiojejunostomy remains the preferred initial treatment method (2). During laparoscopic bile duct exploration surgery (3), macroscopic observation of the liver and extrahepatic biliary tract, together with laparoscopic cholangiography data, forms the basis of the diagnostic and therapeutic approach used by pediatric surgeons. However, through the distal opening of the common bile duct, limited information can be gathered, particularly in terms of evaluating bile duct dysplasia and BA. Therefore, performing an immediate pathological evaluation on intraoperative hepatic sections may be useful for improved diagnostic and surgical management. Here we compare our experience of using frozen liver tissue biopsies and paraffin-embedded sections while using a novel evaluation method for grading BA liver pathological damage.

MATERIALS AND METHODS

Materials

A total of 81 patients with documented BA were collected from September 2010 to August 2013, and liver tissue was collected from patients who underwent sur-

Address for Correspondence: Wenping Yang E-mail: ywp07912000@163.com
Received: November 09, 2015 **Accepted:** January 25, 2016
 • Available online at www.turkjgastroenterol.org • DOI: 10.5152/tjg.2016.15316

gery for BA at the Children's Hospital of our province. Signed informed consent was obtained from all study participants' guardians. Ethical approval was given by the Regional Ethical Vetting Board in Jiangxi Children's Hospital with the registration number 20090535. Diagnosis depended on clinical history, liver function test results, ultrasound examination results, biliary magnetic resonance images, laparoscopic exploratory surgery with intraoperative cholangiography, and liver pathological evaluation results. Hepatitis virus A or C was excluded. For each patient, a written informed consent was obtained from his/her family.

Biochemical tests

Liver function tests comprised bilirubin (TBIL) and conjugated bilirubin (DBIL), gamma-glutamyl transpeptidase, and transaminases (alanine aminotransferase, ALT, and aspartate aminotransferase, AST). In addition, cytomegalovirus (CMV) antibodies (IgMs) were assessed in each patient.

Pathological examination

Pathological examinations were performed on both frozen sections and paraffin-embedded sections (the liver tissue was fixed with 4% neutral formalin, followed by routine dehydration and embedding in paraffin). Serial sections of 4 μm thickness were obtained. Hematoxylin–eosin (HE), Masson, reticular fiber, and immunohistochemical staining were assessed by two highly qualified pathologists (WY and YWP). The liver tissue sections contained an average of 10 portal areas (range, 7-12), for a global depth of 3-5 mm.

Immunohistochemistry

The immunohistochemical study used the streptavidin peroxidase (SP) conjugation method, with the following antibodies: Cytokeratin 19 (CK19), CD68, Smooth Muscle Actin-α (SMA), cytomegalovirus (CMV), Epstein–Barr virus (EBV), Human anti-hepatitis B virus surface antibody, and Human hepatitis B core antigen antibody, which were purchased from Dako Co., Ltd. (Beijing, China). Phosphate-buffered saline replaced primary antibodies as the negative controls. 3,3'-Diaminobenzidine was used for coloration.

Diagnostic criteria

Liver fibrosis was assessed using the standard METAVIR grading method (4): F0, no fibrosis; F1, mild fibrosis in the portal area; F2, mild bridging fibrosis in the adjacent portal area; F3, severe bridging fibrosis in the adjacent portal area; and F4, cirrhosis and annular fibrosis with nodule formation.

To evaluate the small bile duct hyperplasia surrounding the portal areas, the following classification system was used: mild (B1): mild small bile duct hyperplasia in the portal area and the edge of the lobule, discontinuous distribution; moderate (B2): marked hyperplasia in the portal area and the edge of the lobule, with continuous distribution and lobular extension, with the formation a 2–3-layer structure; and severe (B3): same lesions as B2 but with more than three layers or net-like structures.

Liver tissue inflammation was evaluated as follows: mild (G1): small infiltration of lobules and/or portal areas with dotted liver cell necrosis; moderate (G2): marked infiltration of lobules and/or portal areas with focal liver cell necrosis; and severe (G3): severe infiltration of lobules and/or portal areas with liver abscess formation.

Multinucleated giant cell assessment was as follows: none (–); mild (+), occasional multinucleated giant cells; moderate (++), several multinucleated giant cells; and severe (+++), diffuse multinucleated giant cells. Bile plugs in the portal area were reported as absent (–) or present (+).

Statistical analysis

SPSS 17.0 (SPSS Inc.; Chicago, IL, USA) was used for the statistical analyses. The correlation analyses used the Spearman rank correlation, and rank data were compared using the Kruskal–Wallis H test. The Kappa consistency test was used to compare data: Kappa values ≥0.75 indicated good consistency, while 0.75>Kappa≥0.4 indicated ordinary consistency, and Kappa<0.4 indicated poor consistency.

RESULTS

Bioclinical data

All the patients (41 males and 40 females) presented with postnatal persistent obstructive jaundice, with clay-like white stools. The following parameters were measured: TBIL, 194.8±63.0 μmol/L (range, 85–471.9 μmol/L); CBIL, 155.9±48.1 μmol/L (range, 77–382.8 μmol/L); ALT, 158.7±109.9 IU/L (range, 15–782 IU/L); and AST, 277.9±127.5 IU/L (range, 54–744 IU/L). CMV/IgM was positive in 27 cases, and the patient age at the time of surgery ranged from 35 to 150 days (Table 1).

Laparoscopic data

Fibrosis and undeveloped cystic ducts were noticed in 53 cases. In addition, the gallbladder was always present, but with different forms and sizes. In 21 cases, the upper part of the hepatic duct was not visualized by cholangiography. In seven cases, despite the presence of the gallbladder, the cystic duct was obstructed.

Pathological observations

Liver fibrosis

The portal areas showed varying degrees of fibrosis, but fibrous septa were usually broad with a lobular extension or nodule formation (Figure 1). The fibrosis grade was F1 in 1 case, F2 in 11 cases, F3 in 51 cases, and F4 in 18 cases (Table 1). There was not a statistical correlation between the degree of fibrosis and age (r=0.057, p=0.520).

Proliferation of small bile ducts

The 81 cases displayed varying degrees of small bile duct hyperplasia between the portal areas and lobules, accompanied by proliferation of the fibrous tissue with interlobular extension.

Table 1. Relationship between biliary atresia pathological stage and bioclinical parameters

		Degree of inflammation			Proliferation of small bile duct			Liver fibrosis			
	n	G1	G2	G3	B1	B2	B3	F1	F2	F3	F4
Parameter	**81**	**40**	**41**	**0**	**21**	**41**	**19**	**1**	**11**	**51**	**18**
Age											
35–60 days	25	15	10		7	12	6	1	3	16	5
61–90 days	35	17	18		11	16	8	0	6	22	7
≥91 days	21	8	13		3	13	5	0	2	15	6
TBIL (μmol/L)											
<100	2	1	1		0	2	0	0	1	1	0
≥100; ≤200	45	28	17		12	21	12	1	8	24	12
>200	34	11	23		9	18	7	0	2	26	6
CBIL (μmol/L)											
<100	9	4	5		1	7	1	1	2	4	2
≥100; ≤200	57	31	26		16	25	16	0	7	36	14
>200	15	6	9		4	9	2	0	2	11	2
ALT (IU/L)											
<150	49	28	21		12	26	11	1	9	28	11
≥150	32	12	20		9	15	8	0	2	21	7
GGT (IU/L)											
<500	41	19	22		10	22	9	1	8	27	5
≥500; ≤1000	27	15	12		8	13	6	0	2	18	7
≥1000	13	6	7		3	6	4	0	1	6	6

TBIL: total bilirubin; CBIL: unconjugated bilirubin; ALT: alanine aminotransferase; GGT: gamma-glutamyl transpeptidase

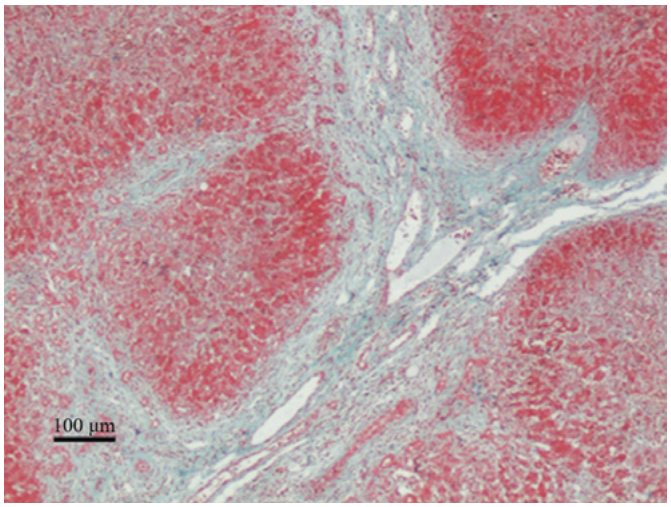

Figure 1. Comprehensive evaluation of severity and BA stage (G1B2F4, Masson staining, ×200 magnification)

The small bile duct morphology was abnormal, showing different aspects, such as C, X, or S shapes; in addition, CK19 was expressed (Figure 2). The severity of small bile duct hyperplasia

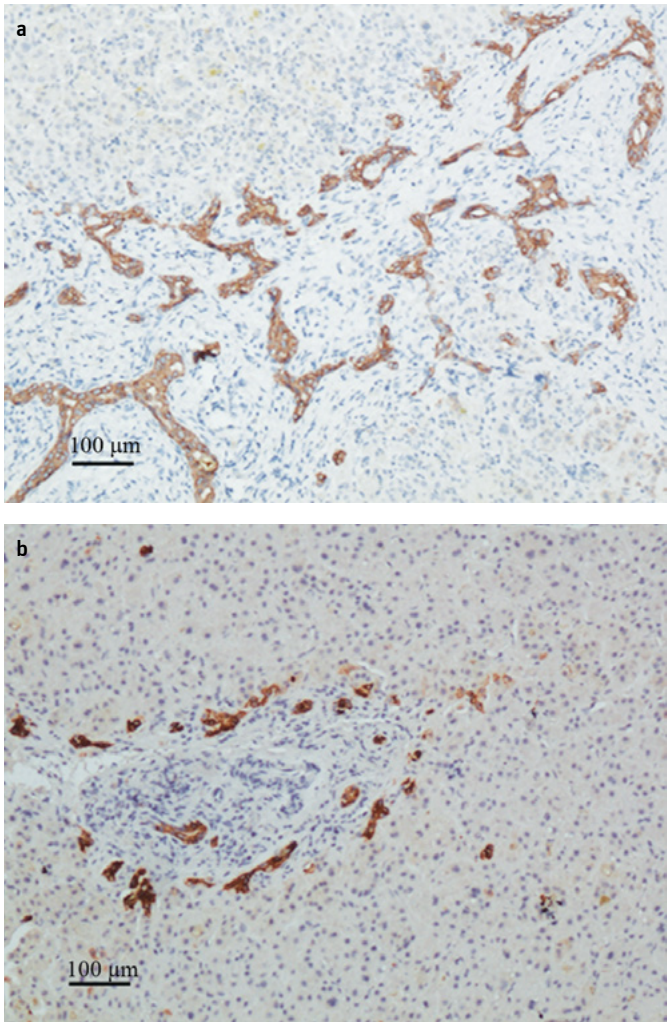

Figure 2. a, b. Immunohistochemistry experiments with the CK19 antibody showing small bile duct hyperplasia and deformity with fibrous tissue hyperplasia in the portal area. BA stage of G1B3F3 (a), BA stage of G1B1F1; SP staining, ×100 magnification (b)

was as follows: mild (B1), 21 cases; moderate (B2), 41 cases; and severe (B3), 19 cases. All 81 cases showed different degrees of liver cell cholestasis; and in 72 cases (88.9%), bile plugs were visible in the small bile ducts of the portal area. Liver fibrosis was statistically positively correlated with the severity of small bile duct proliferation (r_s=0.501; p<0.001) (Table 2).

Inflammatory lesions

Portal infiltration, mainly with lymphoid mononuclear cells, eosinophils, plasma cells, and macrophages, was minimal in the 81 cases. A small amount of lymphatic cells in the lobular extension and the infiltration of mononuclear cells and microabscesses were also observed (Figure 3a). Sixty-four cases (79%) had multiple nuclear giant hepatocytes, which were mild in 36 cases and moderate to severe in 28 cases. There was a statistical correlation between the presence of multinucleated giant liver cells and serum CMVIgM positivity (χ^2=7.914, p=0.019) (Table 3). The liver inflammation severity level was mild in 40 cases (49.4%), moderate in 41 cases (50.6%), and severe in 0 cases. There were no correlations between the extent of inflammation and the de-

gree of liver fibrosis (r_s=–0.07, p=0.952) as well as to the degree of small bile duct proliferation (r_s=–0.07, p=0.533). In 62 cases (76.5%), the interlobular vein structure was not clear, the lumen was small or slit-like, the interlobular artery wall was thickened, and the lumen was stenotic (Figure 3b).

Comparison of the intraoperative frozen and postoperative paraffin-embedded section pathologies

All 81 cases benefited from a quick intraoperative diagnosis, including 2 cases where the intraoperative diagnosis of BA was uncertain. The overall diagnostic accuracy was 97.5%. A relatively good agreement was found between the frozen and paraffin-embedded sections with regard to the degree of small bile duct proliferation (Kappa=0.555; p<0.001), the degree of fibrosis (Kappa=0.574; p<0.001), the degree of inflammation, (Kappa=0.655; p<0.001) (Figure 4), and the degree of bile plugs in the portal area, (Kappa=0.767; p<0.001) (Figure 5). However, for the multinucleated giant cell evaluation, the agreement was poor (Kappa=0.186, p=0.007) (Table 4).

Table 2. Relationship between small bile duct proliferation and liver fibrosis

		Proliferation of small bile ducts			
Liver fibrosis	**n**	**B1**	**B2**	**B3**	**p**
F1	1	1	0	0	
F2	11	6	5	0	
F3	51	13	30	8	<0.001
F4	18	1	6	11	
	81	21	41	19	

Table 3. Relationship between multinucleated giant hepatocytes and CMV infection

		Multinucleated giant hepatocytes				
CMV Test	**Cases**	**–**	**+**	**++**	**+++**	**p**
CMVIgM+	27	2	12	9	4	0.019
CMVIgM–	37	12	17	6	2	
Not done	17	3	7	6	1	

CMVIgM: cytomegalovirus IgM

DISCUSSION

The pathogenesis of BA remains unclear. Multiple factors may lead to progressive inflammation as well as to obstruction and destruction of the bile duct, resulting in biliary cirrhosis. Hepatic pathological features correspond to small bile duct hyperplasia, cholangitis, cholestasis in the portal areas, and interlobular septa with progressive fibrosis in the hepatic plates and portal areas (5). Cocjin et al. (6) performed double staining of the proliferating cell nuclear antigen (PCNA) and anti-pan cytokertain antibodies (AE1/AE3) and concluded that hepatocytes undergo metaplasia to form ductular cells during fetal development and that there is also no ductular cell replication in fetal livers. The plate phenotypic switch to ductules and replication of the ductular cells play a role in the progression to biliary cirrhosis. In addition, Yamaguti et al. (7) performed pathological morphology and immunohistochemical studies for the markers CK7, CK19, and CK8 and dual-labeled with PCNA in 35 cases of BA; their results showed obvious bile duct hyperplasia in the hepatic plates and portal areas. The lobular bile ducts expressed CK7 and CK19, supporting that bile duct hyperplasia corresponds to derived hepatocyte metaplasia. A total of 43% of the cases presented with biliary obstruction, and 20% presented with a reduction in the lobular bile duct. They also found that 29% of the cases exhibited ductal plate malformation and 9% of the cases had ductal plate malformation associated with decreased lobular bile ducts. Moreover, Low et al. (8) reported that 38% of BA cases showed ductal plate malformation, pointing out that BA occurs in the embryonic period. It has also been reported that small bile duct hyperplasia in the portal areas induces liver fibrosis (9).

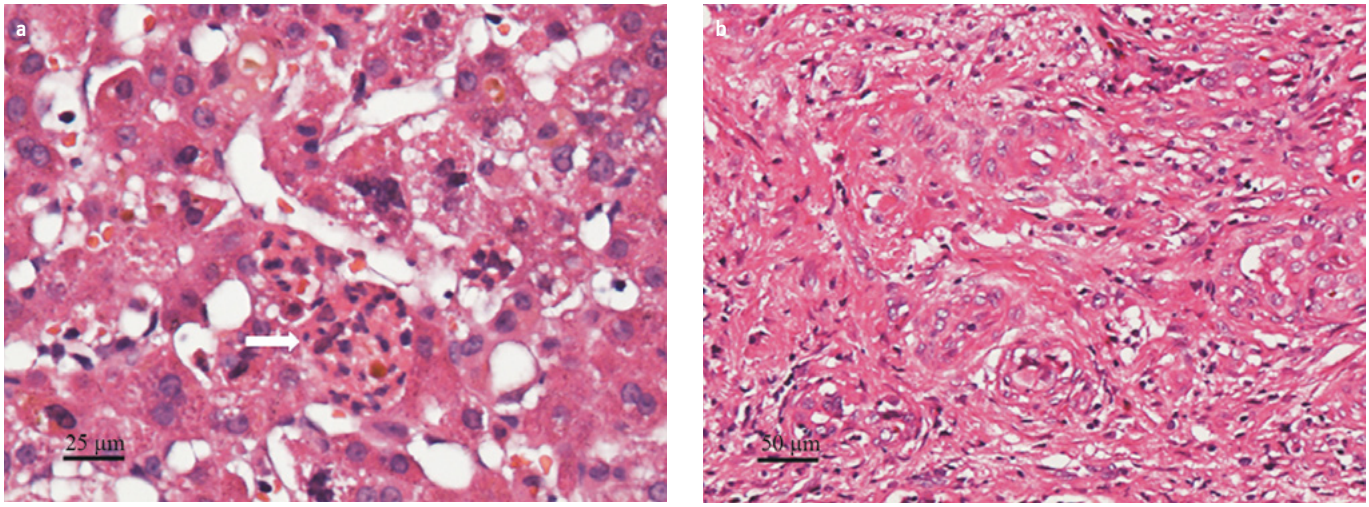

Figure 3. a, b. Inflammatory lesions. Multinucleated giant liver cells and microabscess formation (HE staining, ×400 magnification) (a), vascular morphological changes in the portal area (HE staining, ×200 magnification) (b)

Table 4. Comparisons between intraoperative frozen and postoperative paraffin-embedded liver tissue pathology data

Term	Frozen sections	Paraffin-embedded sections	Statistical analysis
Liver fibrosis	81	81	Kappa=0.574
F1	0	1	p<0.001
F2	11	11	
F3	59	51	
F4	11	18	
Small bile duct proliferation			Kappa=0.555
			p<0.001
B1	6	21	
B2	54	41	
B3	21	19	
Multinucleated giant cells			Kappa=0.186
			p=0.007
–	29	17	
+	36	36	
++	13	21	
+++	3	7	
Liver tissue inflammation			Kappa=0.655
			p<0.001
G1	48	40	
G2	33	41	
G3	0	0	
Bile plugs in portal area			Kappa=0.767
			p<0.001
–	14	18	
+	67	63	

Small biliary epithelial and hepatic cells can secrete a large number of transforming growth factor beta (TGF-β), which in turn activates hepatic stellate cells (HSCs). Activated HSCs produce a large amount of collagen I and IV fibers, which are deposited in the portal areas, leading to progressive liver fibrosis (10). Indeed, activated HSCs transform into myofibroblast-like cells and fibroblasts, resulting in increased synthesis and decreased degradation of the extracellular matrix, finally causing liver fibrosis. Recent studies have reported that TGF-β can cause an epithelial-mesenchymal transition (EMT) in adult liver cells and bile duct epithelial cells *in vitro* (11). Bile duct epithelial cells in living tissues can also participate in portal area fibrosis through EMT (12). EMT also plays an important role in BA liver fibrosis (13). It has also been proposed that hyaline cartilage at the portal plate and squamous epithelium within biliary ductules cause defective morphogenesis, supporting the view that BA may be due to disordered embryogenesis. Alternatively, squamous epithelium in biliary ductules can reflect an unusual metaplastic response to inflammation (14). For example, as reported by Zhou et al. (9), there is a correlation between the proliferation of small bile ducts in BA and liver fibrosis development. Thus, BA progressive liver fibrosis remains the main reason for the postoperative failure of the Kasai surgical procedure and also represents a major indication for liver transplantation.

At present, the degree of BA pathological damage remains based on the viral hepatitis fibrosis (METAVIR) (4) staging system or on Ohkuma's classification, methods which do not take into account the characteristic bile duct abnormalities and inflammation of BA (15). Moreover, in advanced BA with major fibrosis, small bile ducts often appear stunted and reduced due to EMT. Therefore, in the present study, in an effort to integrate the peculiar pathological features of BA, we proposed a grading system that appears to be efficient.

A further important aspect of our work was to evaluate intraoperative frozen sections for pathological assessment. This technique permits a quick diagnostic assessment within 15 min. Moreover, in terms of small bile duct proliferation and fibrosis evaluation, the data obtained were in close agreement (97%) with those obtained with the more commonly used paraffin-embedded sections. In bile bolt and liver cells, cholangiolar cholestasis was clearly seen in the frozen sections, even more clearly than in the paraffin-embedded sections. In particular, periportal bile bolts were the characteristic diagnostic feature for diagnosing BA. A liver biopsy is frequently performed before Kasai surgery. However, in our whole series, no preoperative liver biopsy was performed; nevertheless, BA could be successfully diagnosed. By taking small intraoperative frozen sections of liver tissue for pathology, we were able to evaluate the severity of liver disease within 15 min. Overall, this technique is beneficial for surgeons to improve their diagnostic approach and surgical strategy.

However, the frozen sections had a poor consistency compared to the paraffin-embedded sections on displaying liver tissue multinucleated giant liver cells; therefore, CMV infection diagnosis requires caution with this technique. There is a close link between BA and CMV infection. Since Rauschenfels et al. (16) proposed that BA is due to virus-induced bile duct tree damage, several studies have supported this view by showing the relationship between BA and hepatotropic virus infection, particularly including CMV, reovirus, rotavirus, and papilloma virus. Despite the typical pathological features of CMV infection comprising giant cells and inclusion bodies, they are not easily detected in liver tissue samples of BA patients (17). CMV inclusion bodies were not seen in our 81 cases, but the detection rate of multinucleated giant hepatocytes was 79%, corresponding to 92.6% of the serum CMV IgM-positive cases. However, these giant hepatocytes, usually in small amounts, were also observed in 67.6% of the serum CMV IgM-negative

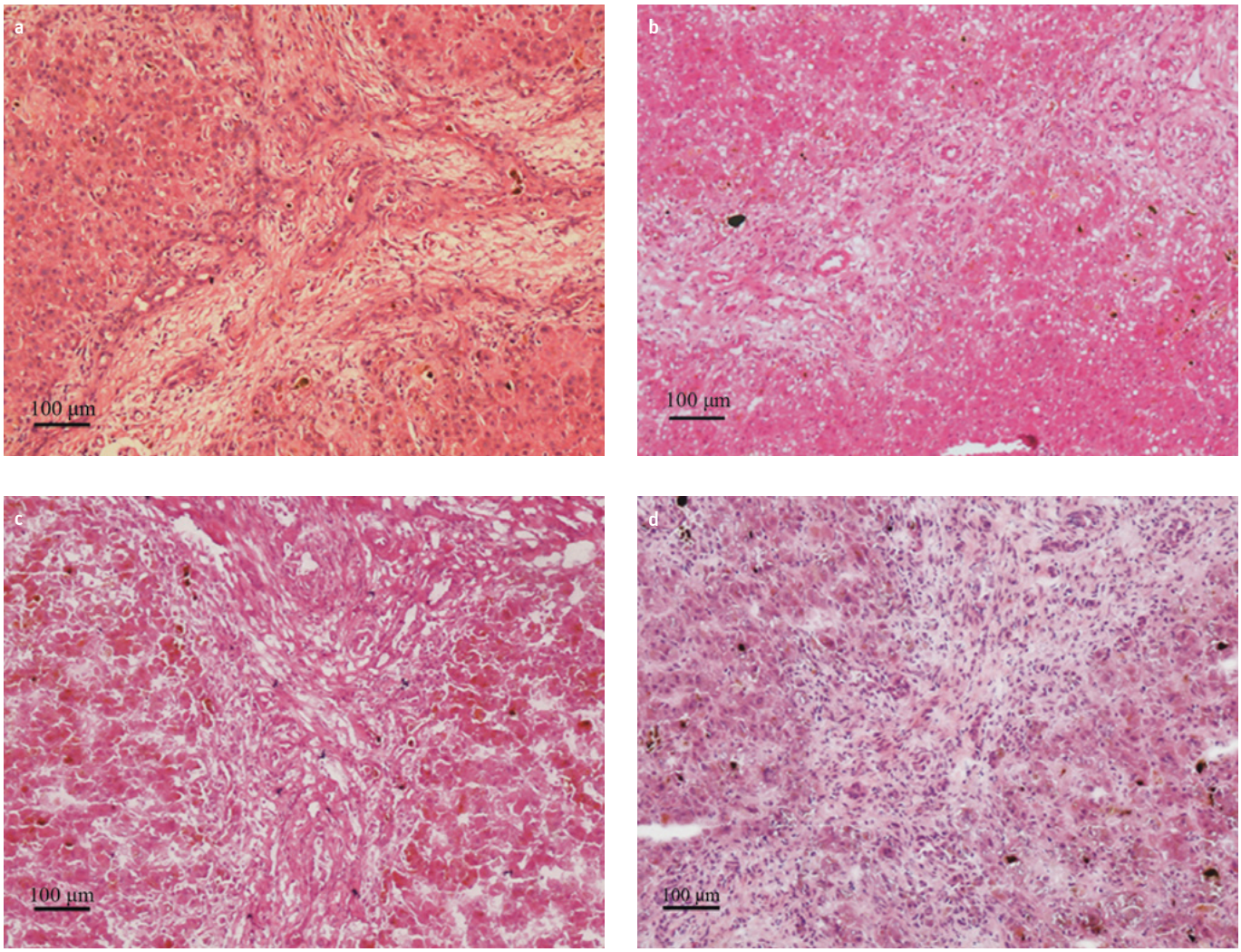

Figure 4. a-d. Staining showing different levels of hyperplasia, fibrosis, and inflammation. Small bile duct hyperplasia with fibrous tissue hyperplasia in the portal area (BA stage: G1B2F3, HE staining, ×100 magnification) (a), frozen section showing moderate hyperplasia in the small bile duct (BA stage: G1B2F2, ×100 magnification) (b), frozen section showing a fibrosis level of F3 (BA stage: G1B2F3, ×100 magnification) (c), frozen section showing an inflammation level of G2 (BA stage: G2B1F2, ×100 magnification) (d)

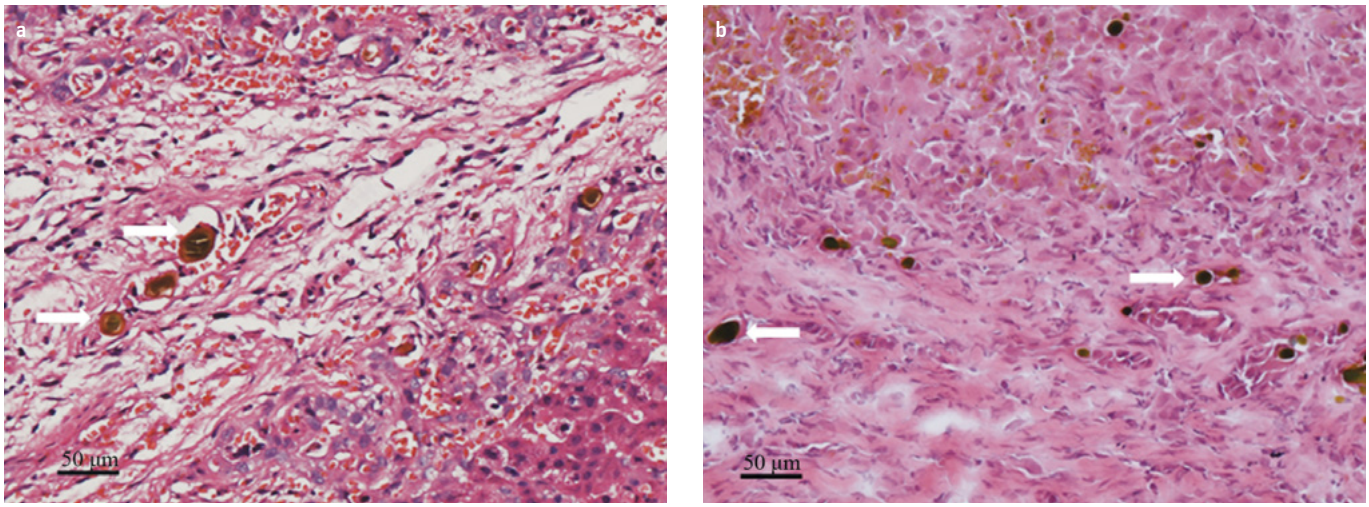

Figure 5. a, b. Bile plugs in the interlobular bile duct; Paraffin-embedded section; HE staining, ×200 magnification (a), frozen section; ×200 magnification (b)

cases, indicating the importance of liver pathology for diagnosing CMV infection. Using fluorescence quantitative polymerase chain reaction, Zhan et al. (18) reported that in their series of 85 BA cases, 60% were CMV-positive, 5.9% were adenovirus (ADV)-positive, and 5% were EBV-positive.

In conclusion, in our series of 81 BA patients, we described the hepatic pathology profile using a novel grading system more adapted to the specificities of hepatobiliary abnormalities in this disease. We also showed, with some limitations regarding the diagnosis of CMV infection, the usefulness of studying intraoperative frozen sections as an adjunct to the more commonly used postoperative paraffin-embedded sections.

Ethics Committee Approval: Ethics committee approval was received for this study from the ethics committee of Jiangxi Children's Hospital (Number: 20090535).

Informed Consent: Written informed consent was obtained from patients who participated in this study.

Peer-review: Externally peer-reviewed.

Author Contributions: Concept - W.Y., J.H.; Design - W.Y.; Supervision - Q.T.; Funding - S.Z.; Materials - Y.W., J.H.; Data Collection and/or Processing - S.Z., Z.L.; Analysis and/or Interpretation - Q.T.; Literature Review - W.Y.; Writer - S.Z., Y.W.; Critical Review - W.Y., J.H.; Other - Z.L.

Conflict of Interest: No conflict of interest was declared by the authors.

Financial Disclosure: The authors declared that this study was supported by the grants from the National Natural Science Foundation of China (No. 81460118).

REFERENCES

1. Fischler B, Haglund B, Hjern A. A population-based study on the incidence and possible pre- and perinatal etiologic risk factors of biliary atresia. J Pediatr 2002; 141: 217-22. [CrossRef]
2. Wildhaber BE. Biliary atresia: 50 years after the first kasai. ISRN Surg 2012; 2012: 132089. [CrossRef]
3. Esteves E, Clemente Neto E, Ottaiano Neto M, Devanir J Jr, Esteves Pereira R. Laparoscopic Kasai portoenterostomy for biliary atresia. Pediatr Surg Int 2002; 18: 737-40.
4. Bedossa P, Poynard T. An algorithm for the grading of activity in chronic hepatitis C. The METAVIR Cooperative Study Group. Hepatology 1996; 24: 289-93. [CrossRef]
5. Sebire IN, Malone M, Ashworth M. Diagnostic Pediatric Surgical Pathology. Churchill Livingstone 2009: 281-2.
6. Cocjin J, Rosenthal P, Buslon V, et al. Bile ductule formation in fetal, neonatal, and infant livers compared with extrahepatic biliary atresia. Hepatology 1996; 24: 568-74. [CrossRef]
7. Yamaguti DC, Patricio FR. Morphometrical and immunohistochemical study of intrahepatic bile ducts in biliary atresia. Eur J Gastroenterol Hepatol 2011; 23: 759-65. [CrossRef]
8. Low Y, Vijayan V, Tan CE. The prognostic value of ductal plate malformation and other histologic parameters in biliary atresia: an immunohistochemical study. J Pediatr 2001; 139: 320-2. [CrossRef]
9. Zhou L, Jin L, Li GS, Liu JC, Hou JH, Yang N. Ductal proliferation induces liver fibrosis in the early stage of biliary atresia. Chin J Pediatr Surg 2005; 26: 281-4.
10. Lamireau T, Le Bail B, Boussarie L, et al. Expression of collagens type I and IV, osteonectin and transforming growth factor beta-1 (TGFbeta1) in biliary atresia and paucity of intrahepatic bile ducts during infancy. J Hepatol 1999; 31: 248-55. [CrossRef]
11. Kaimori A, Potter J, Kaimori JY, Wang C, Mezey E, Koteish A. Transforming growth factor-beta1 induces an epithelial-to-mesenchymal transition state in mouse hepatocytes in vitro. J Biol Chem 2007; 282: 22089-101. [CrossRef]
12. Rygiel KA, Robertson H, Marshall HL, et al. Epithelial-mesenchymal transition contributes to portal tract fibrogenesis during human chronic liver disease. Lab Invest 2008; 88: 112-23. [CrossRef]
13. Harada K, Sato Y, Ikeda H, et al. Epithelial-mesenchymal transition induced by biliary innate immunity contributes to the sclerosing cholangiopathy of biliary atresia. J Pathol 2009; 217: 654-64. [CrossRef]
14. Stahlschmidt J, Stringer MD, Wyatt J, Davison S, Rajwal S, McClean P. Histologic oddities at the porta hepatis in biliary atresia. J Pediatr Surg 2008; 43: 1328-32. [CrossRef]
15. Fumino S, Higuchi K, Aoi S, Furukawa T, Kimura O, Tajiri T. Clinical analysis of liver fibrosis in choledochal cyst. Pediatr Surg Int 2013; 29: 1097-102. [CrossRef]
16. Rauschenfels S, Krassmann M, Al-Masri AN, et al. Incidence of hepatotropic viruses in biliary atresia. Eur J Pediatr 2009; 168: 469-76. [CrossRef]
17. Tarr PI, Haas JE, Christie DL. Biliary atresia, cytomegalovirus, and age at referral. Pediatrics 1996; 97: 828-31.
18. Zhan RZ, Ou ZY, Yu JK, Xu Y, Xian HM. Relationship between human cytomegalovirus infection and biliary atresia. Chin J Pediatr Surg 2010; 31: 653-6.